



# City Research Online

## City St George's, University of London

**Citation:** Hu, H., Zhang, H., Zhou, L., Xu, Y., Lu, L., Chen, J. & Rahman, B. M. (2018). Non-volatile optical memory based on a slot nanobeam resonator filled with GST material. 2018 Asia Communications and Photonics Conference (ACP), doi: 10.1109/ACP.2018.8596243 ISSN 2162-108X doi: 10.1109/ACP.2018.8596243

This is the accepted version of the paper.

This version of the publication may differ from the final published version. To cite this item please consult the publisher's version.

**Permanent repository link:** <https://openaccess.city.ac.uk/id/eprint/21966/>

**Link to published version:** <https://doi.org/10.1109/ACP.2018.8596243>

**Copyright and Reuse:** Copyright and Moral Rights remain with the author(s) and/or copyright holders. Copies of full items can be used for personal research or study, educational, or not-for-profit purposes without prior permission or charge, unless otherwise indicated, provided that the authors, title and full bibliographic details are credited, a hyperlink and/or URL is given for the original metadata page and the content is not changed in any way. For full details of reuse please refer to [City Research Online policy](#).

# Non-volatile optical switch based on a GST-loaded directional coupler

Hanyu Zhang, Linjie Zhou, Liangjun Lu, and  
Jianping Chen

Shanghai Institute for Advanced Communication and  
Data Science, Shanghai Key Lab of Navigation and  
Location Services, State Key Laboratory of Advanced  
Optical Communication Systems and Networks  
Department of Electronic Engineering, SJTU  
Shanghai, China  
[ljzhou@sjtu.edu.com](mailto:ljzhou@sjtu.edu.com)

**Abstract**—We present a non-volatile optical switch based on a directional coupler comprising a silicon-Ge<sub>2</sub>Sb<sub>2</sub>Te<sub>5</sub>(GST) hybrid waveguide. The non-volatility of GST makes it attractive for reducing static power consumption in optical switching. Experimental results show that the optical switch has an extinction ratio of >20 dB in the bar state and >25 dB in the cross state around 1578 nm wavelength. The insertion loss is 2 dB and 7 dB for the bar and cross states, respectively.

**Keywords**—silicon photonics; phase change material; directional coupler

## I. INTRODUCTION

A directional coupler (DC) is a basic component in integrated photonics that couples light propagating in a waveguide to another parallel waveguide placed in close proximity. The operation principle of the DC can be explained by the coupled mode theory. It has been widely used in optical switches [1], multiplexers/de-multiplexers [2] and polarization beam splitters [3] etc. On the other hand, tunable silicon photonic devices are based primarily on the thermo-optic (TO) effect or the free carrier dispersion effect (FCD). They are both volatile and require constant power to maintain tuning. The power consumption can be reduced considerably, if the refractive index change can be maintained using a non-volatile tuning method.

Phase change materials (PCMs) have a striking portfolio of properties [4]. They can be rapidly and reversibly switched between amorphous (*am*) and crystalline (*cr*) states. The Ge<sub>2</sub>Sb<sub>2</sub>Te<sub>5</sub> (GST) material, as a PCM commonly used in optical storage, exhibits distinct optical (refractive index) and electrical (resistance) properties between its amorphous and crystalline states [5]. Besides, its phase change is reversible and does not degrade material properties after multiple phase transitions [6]. In addition, this material possesses the “self-holding” feature [7], and consequently there is no need for static power consumption to maintain the states. Hence, this feature can be utilized to manipulate light propagation and implement reconfigurable non-volatile optical devices.

In this paper, we demonstrate an optical switch based on a DC. The DC is composed of a silicon waveguide coupled with a GST-loaded silicon waveguide. The propagation constant of the GST-loaded silicon waveguide can be adjusted by changing the GST phase state. We use the finite-

B. M. A. Rahman

Department of Electrical and Electronic Engineering  
City, University of London  
London, U.K.

[B.M.A.Rahman@city.ac.uk](mailto:B.M.A.Rahman@city.ac.uk)

difference eigenmode (FDE) solver to calculate the waveguide mode and three-dimensional finite-difference time-domain (3D-FDTD) method to calculate the optical transmission. Experimental results show that the optical switch can achieve >20 dB extinction ratio (ER) for both switching states around the operation wavelength. The cross state has a higher insertion loss (IL) of 7 dB.

## II. NUMERICAL SIMULATION

Fig. 1 shows the complex refractive index ( $n+ik$ ) of radio-frequency (RF) sputtered GST film in dependence of wavelength, measured by ellipsometry. Reversible switching of GST by optical or electrical pulses has been demonstrated in the literature [4]. It can be seen that due to the significant change in bonding, the refractive index of GST is increased considerably when GST is changed from an amorphous state to a crystalline state [8].

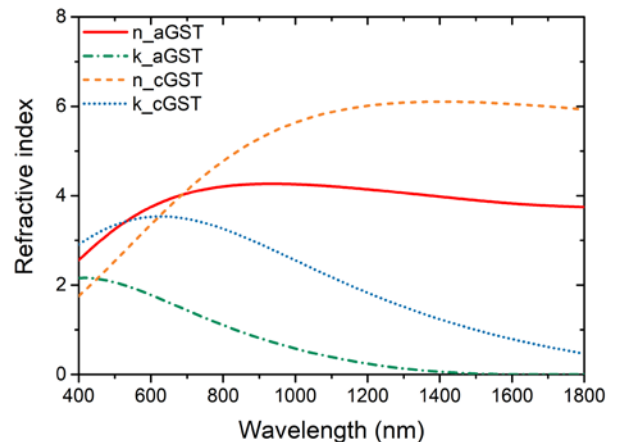


Figure 1. Real and imaginary parts of GST material refractive index changing as a function of wavelength. aGST: amorphous GST; cGST: crystalline GST.

Fig. 2 illustrates the schematic structure of the proposed  $1 \times 2$  optical switch based on a DC. It is composed of a DC in which GST is deposited on top of one silicon waveguide. The inset shows the cross-section of the DC. The GST film thickness is  $T = 40$  nm and width is  $W = 400$  nm. The silicon waveguide height is  $h = 220$  nm. The two waveguides have different widths of  $w_1$  and  $w_2$ , which will be optimized to

achieve the phase matching condition in the *am*-GST state. The under-cladding of the silicon waveguides is SiO<sub>2</sub> and the upper-cladding is air. In our simulation, the refractive indices of silicon and silica are taken as 3.4764 and 1.444, respectively.

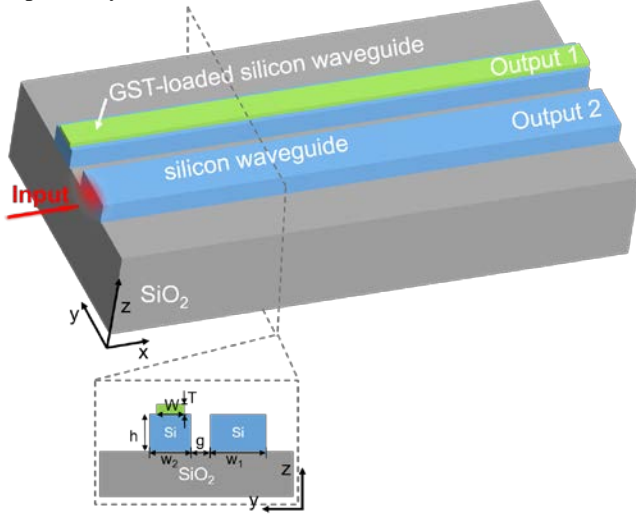


Figure 2. Schematic structure of the optical switch. Inset shows the cross-sectional view of the coupled waveguides.

Fig. 3(a) shows the calculated effective indices of the fundamental transverse electric (TE<sub>0</sub>) and transverse magnetic (TM<sub>0</sub>) optical modes of the silicon waveguide changing with waveguide width  $w_1$  at 1550 nm wavelength. We choose  $w_1 = 500$  nm, corresponding to an effective index of 2.384 for the TE<sub>0</sub> mode as indicated by the dotted line. Fig. 3(b) shows the real effective index of the TE<sub>0</sub> and TM<sub>0</sub> optical modes of the GST-loaded silicon waveguide changing as a function of  $w_2$  when GST is in the *am* and *cr* states. When  $w_2 = 424$  nm, the real effective index of the GST-loaded waveguide is 2.384 for the *am* state, equal to that of the silicon waveguide. The  $E_y$  intensity distributions of the waveguide modes are presented in Fig. 3(c). The optical field is mainly confined in the silicon waveguide when GST is in the *am* state, while it is localized more into the GST layer when it is in the *cr* state. This results in a large difference in their effective indices. Therefore, light can efficiently couple from the silicon waveguide to the GST-loaded silicon waveguide in the *am* state due to the matched propagation constant. When GST is changed to the *cr* state, light can no longer couple to the other waveguide. This is the basic operation principle of the phase-change enabled optical switch.

We set the gap size between the two waveguides to be  $g = 230$  nm. Fig. 4 illustrates the  $E_y$  intensity profiles for the two super-modes of the coupled waveguides. In the *am* state, the two waveguides are strongly coupled, with the super-modes exhibiting an even-mode and an odd-mode. In the *cr* state, however, the two waveguides are weakly coupled, with the super-modes approaching the individual waveguide modes. Table 1 summarizes the extracted refractive indices of the two super-modes.

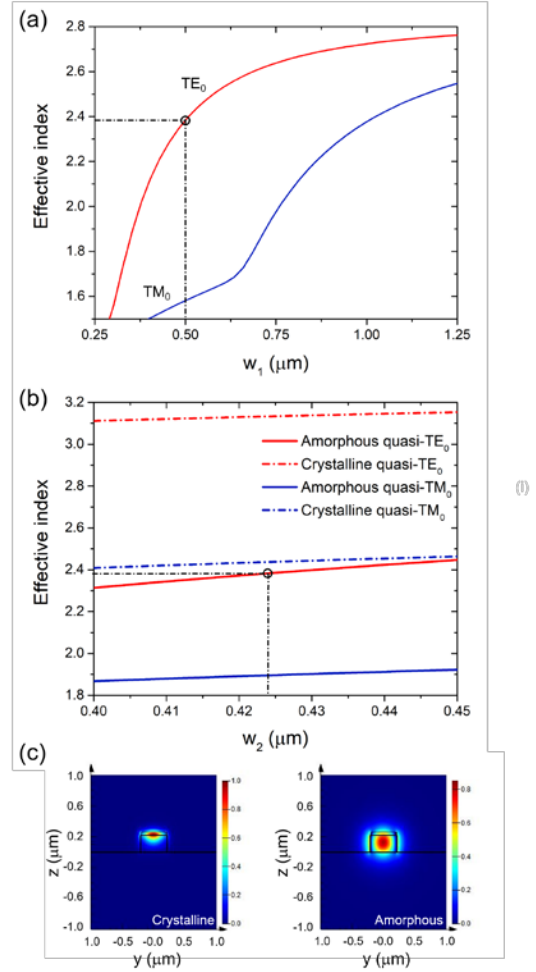


Figure 3. (a) Effective indices of two lowest-order modes in the silicon waveguide. (b) Real effective indices of two lowest-order modes in the GST-loaded silicon waveguide. (c) Waveguide mode  $E_y$  intensity distributions in the GST-loaded silicon waveguide.

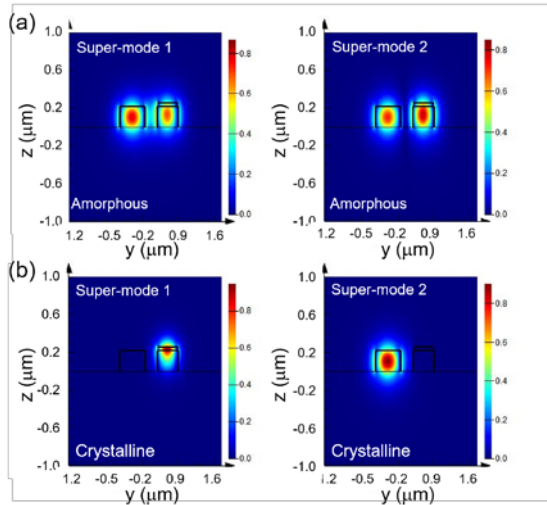


Figure 4. Electric field  $E_y$  intensity distributions in the coupled waveguides when GST is in (a) the amorphous state and (b) the crystalline state.

TABLE 1. EFFECTIVE INDEX OF THE SUPER-MODES IN THE COUPLED WAVEGUIDES.

GST phase	Super-mode 1	Super-mode 2
Amorphous	2.3892+0.000325i	2.3795+0.00042i
Crystalline	3.1342+0.6378i	2.385+3.225e-5i

Fig. 5 (a) and (b) show the simulated light propagation in the coupled waveguide for two GST states. When the GST is amorphous, the two coupled waveguides satisfy the phase matching condition, and the input light launched into the silicon waveguide is evanescently coupled into the GST-loaded silicon waveguide. The cross-over coupling length is 80  $\mu\text{m}$ . When the GST film is crystallized, the input light cannot be coupled into the GST-loaded silicon waveguide and is thus remained in the original silicon waveguide. The simulated transmission spectra are shown in Fig. 5(c). It can be seen that the optimal operation wavelength is around 1578 nm, where the extinction ratio in the *am* state reaches the maximum.

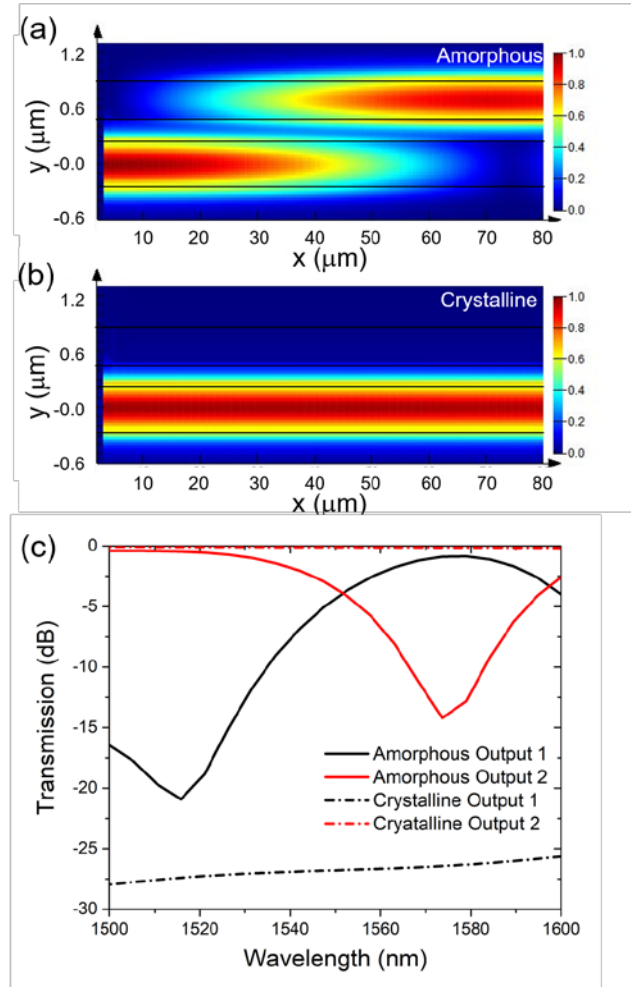


Figure 5. (a, b) Light propagation in the directional coupler when GST is (a) amorphous and (b) crystalline. (c) Transmission spectra of the two output ports in amorphous and crystalline states.

### III. DEVICE FABRICATION

We fabricated the device on a SOI wafer. The wafer was first cleaned by acetone, isopropanol (IPA) and deionized (DI) water in sequence and then baked for 2 minutes at 180  $^{\circ}\text{C}$  temperature. Next, the wafer was spin-coated with ZEP-520 e-beam resist, and prebaked for 3 minutes at 180  $^{\circ}\text{C}$ . We used e-beam lithography to define the silicon waveguide patterns. The e-beam resist was developed in IPA/MIBK (3:1). The pattern was transferred to the silicon layer with inductively-coupled plasma (ICP) dry etch. The residual e-beam resist was completely removed by N-Methyl pyrrolidone (NMP). The GST deposition window was opened using the second e-beam lithography process. A 40-nm-thick GST film was then sputtered on the wafer using an RF sputtering system from a stoichiometric  $\text{Ge}_2\text{Sb}_2\text{Te}_5$  target (20 W, 15 s.c.c.m. Argon gas, 0.0889 nm/min deposition rate). Finally, the lift-off process was used to remove the GST outside the deposition window in a warm acetone bath. Fig. 6 shows the scanning electron microscope (SEM) image of the fabricated device.

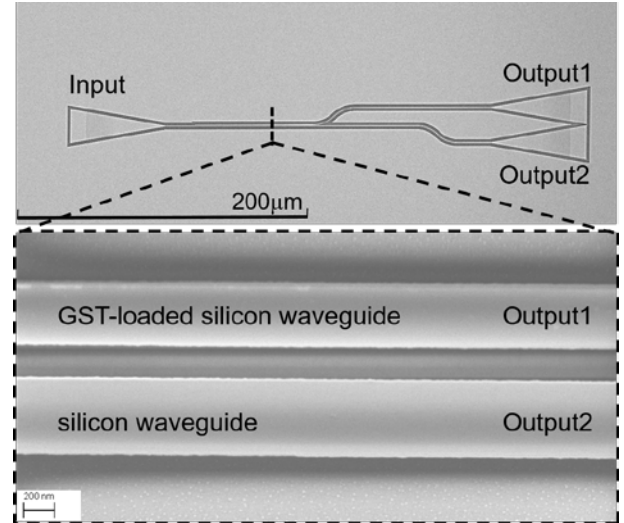


Figure 6. Scanning electron microscope image of the fabricated device. The inset shows the zoom-in of the directional coupler.

### IV. EXPERIMENTAL RESULTS AND DISCUSSION

We measured the transmission spectrum of the device using a tunable continuous-wave (CW) laser scanning from 1500 nm to 1600 nm with a step size of 5 pm. A polarization controller was used to adjust the polarization to TE. Light was coupled in and out of the device through grating couplers by using two single mode fibers. The alignment was precisely adjusted by two 6-axis motorized piezo stages. The grating couplers were designed to be linearly chirped with an etched depth of 70 nm. The measured transmission spectra were all normalized to a reference straight waveguide. Fig. 7 (a) and (b) show the measured spectra from the two output ports when GST is in the crystalline and amorphous states, respectively. It can be seen that the output transmission is wavelength-insensitive when GST is crystalline. It is because the light cannot be coupled to the GST-loaded waveguide.

The bar-port (output 2) insertion loss is around 2 dB with the bandwidth  $>100$  nm. The extinction ratio between the two ports is  $>20$  dB for the 100 nm wavelength range. When GST is amorphous, the coupling is sensitive to wavelength. This is because both the cross-over coupling and the exact phase match can only be achieved at a single wavelength. The maximum transmission of the cross-port (output 1) is achieved at the 1578 nm wavelength. The insertion loss is 7 dB and the maximum extinction ratio is  $>25$  dB.

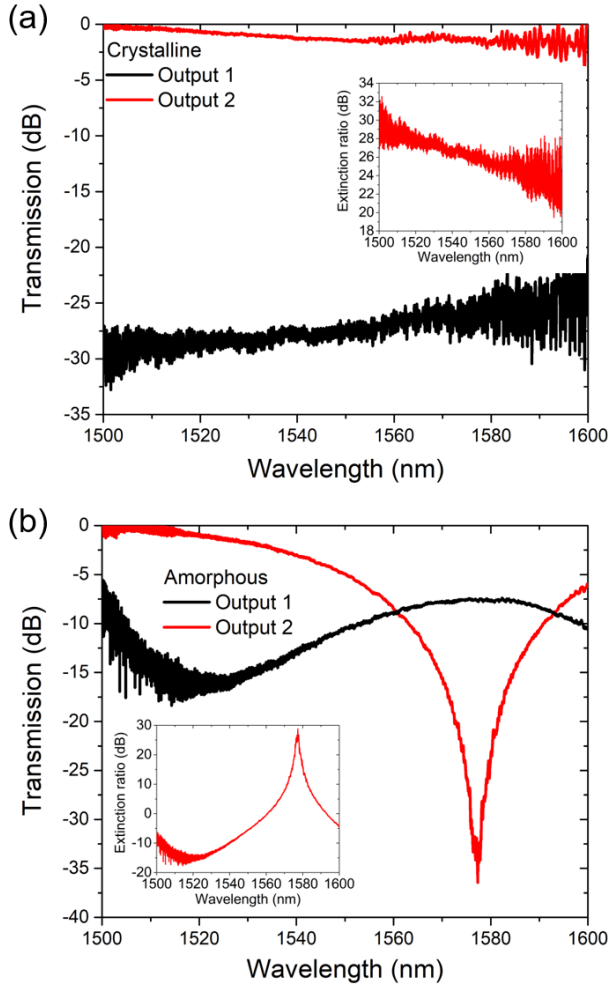


Figure 7. Measured transmission spectra of the device when GST is at (a) crystalline and (b) amorphous states. The insets show the extinction ratio curves.

The insertion loss in the cross state (*am*-GST) is mainly caused by the GST material loss (absorption loss and surface roughness induced scattering loss). In fact, The GST material can be replaced by other low-loss materials, such as GeSe [9] and Ge<sub>2</sub>Sb<sub>2</sub>Se<sub>4</sub>Te<sub>1</sub> [1] etc. They have a lower loss at the 1550 nm wavelength, which are worth further exploration in the future work. In addition, in order to realize a broadband directional coupler, we can design an adiabatic directional

coupler. The width of one waveguide increases while the width of the other waveguide decreases. The phase match condition at different wavelengths can always be satisfied at a certain coupling point along the directional coupler. The coupler length should be longer in order to get efficient coupling.

## V. CONCLUSIONS

We have demonstrated a non-volatile optical switch based on a directional coupler comprising a silicon-GST hybrid waveguide. GST is a phase change material that exhibits a large difference in refractive index between a crystalline state and an amorphous state. In addition, GST's non-volatile nature provides a self-holding feature for the switch, allowing the switch states to be maintained without static power. The directional coupler length is 80  $\mu\text{m}$ . Experimental results exhibit that the optical switch has an ER of  $>20$  dB in the bar state in a wide spectral range and  $>25$  dB in the cross state near the optimal coupling wavelength of 1578 nm. The IL is 2 dB for the bar state and 7 dB for the cross state. The performance can be further improved by using low-loss phase change materials.

## ACKNOWLEDGMENT

This work was supported in part by the National Natural Science Foundation of China (NSFC) (61422508, 61535006, 61705129, 61661130155).

## REFERENCES

- [1] Q. Zhang, Y. Zhang, J. Li, R. Soref, T. Gu, and J. Hu, "Broadband nonvolatile photonic switching based on optical phase change materials: beyond the classical figure-of-merit," *Opt. Lett.*, vol. 43, no. 1, pp. 94-97, 2018.
- [2] W. Jiang, "Ultra-compact and fabrication-tolerant mode multiplexer and demultiplexer based on angled silicon waveguides," *Opt. Commun.*, vol. 425, pp. 141-145, 2018.
- [3] Y. Kim, M. H. Lee, Y. Kim, and K. H. Kim, "High-extinction-ratio directional-coupler-type polarization beam splitter with a bridged silicon wire waveguide," *Opt. Lett.*, vol. 43, no. 14, p. 3241, 2018.
- [4] M. Wuttig, H. Bhaskaran, and T. Taubner, "Phase-change materials for non-volatile photonic applications," *Nat. Photon.*, vol. 11, no. 8, pp. 465-476, 2017.
- [5] J. Feldmann et al., "Calculating with light using a chip-scale all-optical abacus," *Nat. Commun.*, vol. 8, no. 1, p. 1256, 2017.
- [6] M. Stegmaier, C. Ríos, H. Bhaskaran, C. D. Wright, and W. H. P. Pernice, "Nonvolatile all-optical  $1 \times 2$  switch for chipscale photonic networks," *Adv. Opt. Mater.*, vol. 5, no. 1, p. 1600346, 2017.
- [7] S. Raoux, F. Xiong, M. Wuttig, and E. Pop, "Phase change materials and phase change memory," *MRS Bulletin*, vol. 39, no. 08, pp. 703-710, 2014.
- [8] K. Shportko, S. Kremers, M. Woda, D. Lencer, J. Robertson, and M. Wuttig, "Resonant bonding in crystalline phase-change materials," *Nat. Mater.*, vol. 7, no. 8, pp. 653-8, 2008.
- [9] R. Soref, "Phase-change materials for Group-IV electro-optical switching and modulation," 12th International Conference on Group IV Photonics, pp. 157-158, Vancouver, Canada, 2015.